energies

MDPI

Article

Numerical Evaluation of Biochar Production Performance of Downdraft Gasifier by Thermodynamic Model

Donghoon Shin [1], Akhil Francis [2], Purushothaman Vellayani Aravind [3,4], Theo Woudstra [4], Wiebren de Jong [3] and Dirk Roekaerts [3,*]

[1] School of Mechanical Engineering, Kookmin University, Seoul 02707, Korea
[2] St. Joseph's College of Engineering and Technology Palai, Kerala 686579, India
[3] Process & Energy Department, Delft University of Technology, 2628 CN Delft, The Netherlands
[4] Faculty of Science and Engineering, University of Groningen, 9701 BA Groningen, The Netherlands
* Correspondence: d.j.e.m.roekaerts@tudelft.nl

Abstract: A theoretical evaluation of the biochar production process using a biomass gasifier has been carried out herein. Being distinguished from the previous research trend examining the use of a biomass gasifier, which has been focused on energy efficiency, the present study tries to figure out the effect of biochar production rate on the overall process performance because biochar itself has now been given a spotlight as the main product. Biochar can be utilized for agricultural and industrial purposes, along with the benefit of climate change mitigation. A thermodynamic model based on chemical equilibrium analysis is utilized to demonstrate the effect of biochar production rate on the producer gas characteristics such as gas composition, LHV (lower heating value) and cold gas efficiency. Three gasifier models using chemical equilibrium model are reconstructed to simulate biochar-producing gasifiers, and seven kinds of biomass are considered as feed material. Depending on the assumptions applied to the models as well as the biomass types, the results of the simulation show a large variance, whereas the biochar yield rate increases. Through regression analysis with a generalized reduced gradient optimization method, simplified equations to estimate the cold gas efficiency (CGE) and LHV of producer gas of the biochar production process were derived as having six parameters of biomass LHV, fractions of ash, carbon and water, reduction zone temperature, and biochar yield rate. The correlation factors between the thermodynamic model and the regression model are 96.54% and 98.73% for the LHV of producer gas and CGE, respectively. These equations can supply the pre-estimation of the theoretical maximum performance of a planning biochar plant.

Keywords: biomass; biochar; downdraft gasifier; thermodynamic model; correlation equation

Citation: Shin, D.; Francis, A.; Aravind, P.V.; Woudstra, T.; de Jong, W.; Roekaerts, D. Numerical Evaluation of Biochar Production Performance of Downdraft Gasifier by Thermodynamic Model. *Energies* **2022**, *15*, 7650. https://doi.org/10.3390/en15207650

Academic Editor: Dimitrios Kalderis

Received: 13 September 2022
Accepted: 11 October 2022
Published: 17 October 2022

1. Introduction

Due to recent severe climate events, activities searching for a solution to mitigate climate change are globally overwhelming. In this context, 'negative emissions' denoting technologies leading to a net decrease in CO_2 has been proposed as a way to overcome the too-slow pace of in the reduction in CO_2 (or other greenhouse gases)-emitting technologies. The negative emission technology examines the storage of carbon absorbed by biomass in the form of biochar and its possible utilization for industrial purposes [1]. As long as the biochar is not burned, the carbon is captured and stored in a stable condition through the negative emission process. Compared with the well-known CCS (carbon capture and storage) concept [2], the negative emission via biochar process has received positive prospects because of the absence of the risk of storage of CO_2, and the potential economic profit [3]. The biochar has different industrial characteristics depending on the process environment. Fast pyrolysis at high temperature of biomass can be a way to produce high-quality biochar close to activated carbon [4]. Additionally, it is well known that high-temperature biochar produced above 800 °C behaves similar to a catalyst, enabling tar cracking and sequestration of carbon from

various hydrocarbons to generate hydrogen [5–8]. The biochar is also a soil amendment agent with high moisture and fertilizer-holding ability, as well as fertilizer properties [9].

In spite of the potential of biochar for climate change mitigation, little research has been carried out focusing on the biochar production rate in a biomass gasifier. Most of the previous research on biomass gasification was focused on energy of the produced gas [10–13]. A fluidized bed reactor is a popular reactor for small-scale solid particle reaction [10]. Using a fluidized bed as a biomass gasifier provides a good efficiency of gasification reaction but is not suitable for biochar production due to difficulties of separation of biochar from the fluidizing media. On the other hand, using an entrained flow gasifier, which is popular in IGCC (Integrated Gasification Combined Cycle), it is not possible to sequestrate carbon from the molten ash [14]. Therefore, the up- or downdraft fixed-bed gasifier is known to be the best possible facility to produce biochar on a relatively small scale. In particular, the downdraft gasifier has strength of lower tar content in the producer gas (PG) than the updraft type [11]. Most of these biomass gasifiers utilize partial oxidation of biomass to supply heat for pyrolysis and reduction in biomass: approximately 30~40% of stoichiometric air is used to partially oxidize the biomass. However, this oxidation easily generates the problem of slagging of ash blocking the facility if air is not spread well into the bed because the biomass bed is burning fast to result in ash melting, whereas the other part is too cool to react due to lack of oxygen [15,16]. Furthermore, maintaining the uniformity of the partial oxidation reaction in a fixed bed is more difficult as the scale of the gasifier is bigger. Until now, the 2MWth Parma (Italy) downdraft gasifier has been reported as the biggest commercial plant [17], and these gasifiers have been developed with focus on syngas production rather than biochar production [18,19]. So far, most of the biochar-focused production was carried out at a low temperature. For example, the torrefaction process transforms biomass at 200~400 °C into biochar still containing a high volatile content, and the main usage of the biochar is as a fuel source leading to CO_2 emission [20].

The present study uses thermodynamic process simulation by Cycle-Tempo, a commercial software based on chemical equilibrium calculation and suitable for the simulation of various energy plant designs. Altafini et al.'s downdraft gasifier model is one of the earliest of the thermodynamic model to simulate the biomass gasifier. They divide the gasification process into three sub processes, including pyrolysis, oxidation and re-duction [21]. The char production ratio was fixed to 5%, and the focus was on PG properties such as composition and calorific value, depending on the moisture content of the biomass. They also compared other process models composed with two or three gasifier modules and several separators to match the measured PG composition. In a more recent study by Vera et al., two sub gasifier modules were used in series to simulate a 110 kWth gasifier using olive oil farm residues [22]. The first gasifier is for pyrolysis process and the second is for oxidation and the reduction process. Fortunato et al. compared Altafini's and Vera's models to derive an improved version based on Altafini's model [23]. These research results are identified into two major types of biomass downdraft gasification model for application on biochar production. The first one uses two gasifier modules to simulate pyrolysis and oxidation combined reduction, and the second extends the first type by putting the oxidation process between pyrolysis and reduction. By controlling operation parameters such as gasifier temperature, those models showed good similarity in the composition of PG and CGE with the measured data. However, their different configurations could lead to different levels of accuracy.

In the present study, thermodynamic models of a downdraft fixed-bed biomass gasifier were set up based on the literature and utilized to produce simulation data focusing on production rate of biochar. The seven biomasses were considered as the target fuels to find out the operation performance of the biochar production process. Additionally, simple correlation models derived by regression analysis are proposed to estimate the LHV of PG and CGE. Coefficients of the correlation model are determined through regression analysis and error minimization. These regression models can be used for evaluation of biochar

plant performance in a relatively simple way when knowing biomass quality and basic operation conditions, which can be useful to make a first estimate of the economic feasibility.

2. Biomass Resource

Table 1 shows the ultimate and proximate analysis of the biomass listed from India [24–29]. The average LHV of woody biomass is reported to be 15,435 kJ/kg at dry condition. Water and ash contents are important variables affecting LHV of biomass and biochar characteristics. It is obvious that high water content will decrease LHV but increase the levels of hydrogen in PG. The ash also decreases the LHV of PG but increases biochar yield rate because ash tends to remain in the biochar. However, if pure carbon from biochar is preferred, then ash is an unwanted material. Depending on the biochar application, the operation of biochar plant should use an appropriate biomass resource as well as reaction process.

Table 1. Ultimate and proximate analysis of biomass resources [24–29].

Composition	Rice Husk [24]	Paddy Straw [25]	Coconut Shell [26]	Coconut Frond [27]	Torrefied Arecanut Husk [28]	Cassava Stalk [28]	Cassava Rhizome [29]	Average	Standard Deviation
Ca	52.97	53.17	51.21	45.51	57.67	51.13	51.55	51.89	3.61
Oa	38.70	40.23	43.10	47.60	35.62	41.33	40.45	41.00	3.73
Ha	7.28	5.28	5.60	6.02	5.87	6.82	6.69	6.22	0.72
Sa	0.85	0.27	0.10	0.09	0.00	0.06	0.05	0.20	0.30
Na	0.20	1.05	0.00	0.77	0.84	0.66	1.27	0.68	0.45
water	10.4	4.3	4.4	4.2	3.56	15.54	8.31		
ash	18.15	20.49	3.1	6.7	5.19	6.01	4.05		
LHV (kJ/kg)b	13,911	12,802	15,020	12,489	18,340	13,830	15,794		

a: Dry ash free condition. b: Calculated by Dulong equation.

The H composition ratio of biomass is relatively constant, but C and O composition vary and have a clear negative correlation against each other as shown in Figure 1. From this analysis, carbon or oxygen composition ratio can well represent the overall composition of biomass at DAF (dry ash free condition).

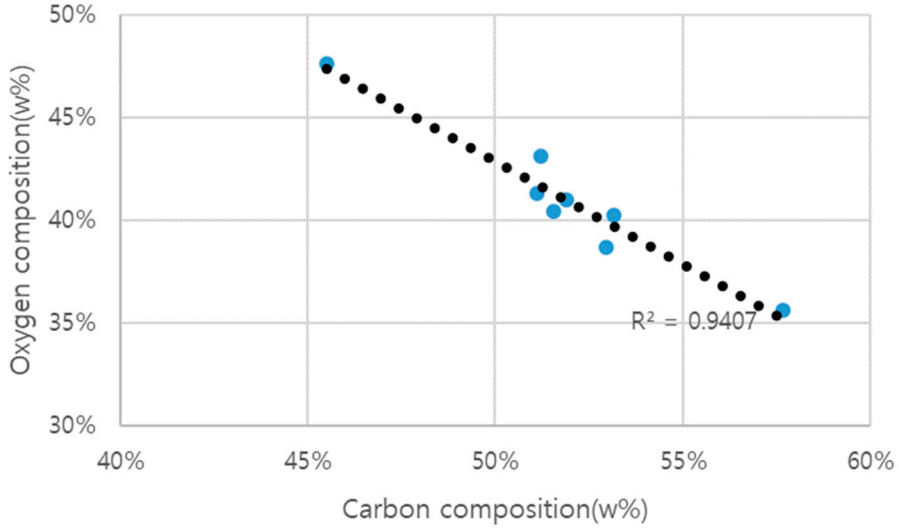

Figure 1. Relation between carbon and oxygen content in biomasses at dry ash free condition.

3. Thermodynamic Models of Downdraft Biomass Gasifier

Previous studies have shown that the chemical equilibrium model is reasonable in spite of having some limitations due to the heterogeneous kinetic reaction in the downdraft biomass gasifier [12,21–23]. Heat and mass transfer in biomass fixed beds are slow phenomena taking from several minutes to an hour, depending on the biomass granule size, as well as the reacting environment. The pyrolysis reaction generating multiple hydrocarbon species, called volatiles, is dependent on the reaction environment of oxidant

supply and temperature. Furthermore, a non-uniform reaction environment in the gasifier is unavoidable for several reasons: (1) Penetration and uniform dispersion of oxidant gas into solid bed is difficult because of strong drag of porous bed. (2) Mixing between oxidant and fuels is difficult due to laminar flow characteristics in bed. (3) Local temperature and chemical composition also are non-uniform in gas media as well as solid media due to reasons (1) and (2). Therefore, the biomass gasifier is, in essence, a heterogeneous reactor in which thermodynamic and fluid dynamics are the governing phenomena, and challenging to simulate with a chemical equilibrium model assuming complete mixing. However, a thermodynamic model has the advantage that it can be based on accurately known property data and is a direct and flexible tool to describe steps in energy conversion. Some aspects of incomplete reaction can be implemented in an equilibrium approach by imposing the bypass stream. Previous studies on the downdraft gasifier have shown that the application of the thermodynamic model has been reasonably chosen as method of approach. The selected two models in this research each have two and three coupled gasification reactors, respectively.

3.1. Two-Reactor Model (Vera)

The reconstructed model of Vera et al. is shown in Figure 2 [22]. It is the simplest method to simulate the downdraft gasifier with high levels of accuracy. In the general biomass gasifier, moisture evaporation, pyrolysis, and char reaction in the solid phase take place sequentially, whereas partial oxidation at pyrolysis zone and reduction at the char reaction zone occur in the gas phase. In Vera's gasifier model, the first reactor (gasifier 3) simulates moisture evaporation and pyrolysis, and the second reactor (gasifier 5) simulates the remaining processes (oxidation and char reaction). The pyrolysis temperature of the first reactor is fixed to be 500 °C, and a bypass (stream 11) is introduced to simulate unconverted carbon (5%) and methane (3%) due to an uneven reaction in the bed, according to the literature [22]. At the second reactor, the oxidant is added to heat up the reduction zone to higher than 1000 °C using an oxidant/fuel ratio. The bypassed carbon and methane join at the exit of the second gasifier module and the biochar is separated afterwards (separator 12). Heat loss to the environment is fixed to be 5% of the biomass energy. The backward heat transfer from the reduction zone to the pyrolysis zone via conduction and radiation heat transfer is implemented by a fictitious steam flow (source 1 to sink 7) to maintain the first gasifier exit temperature at 500 °C. After transferring heat at the first gasification reactor, the steam continues to the second gasification reactor to return to the start condition; thus, the net heat transfer to the environment is zero.

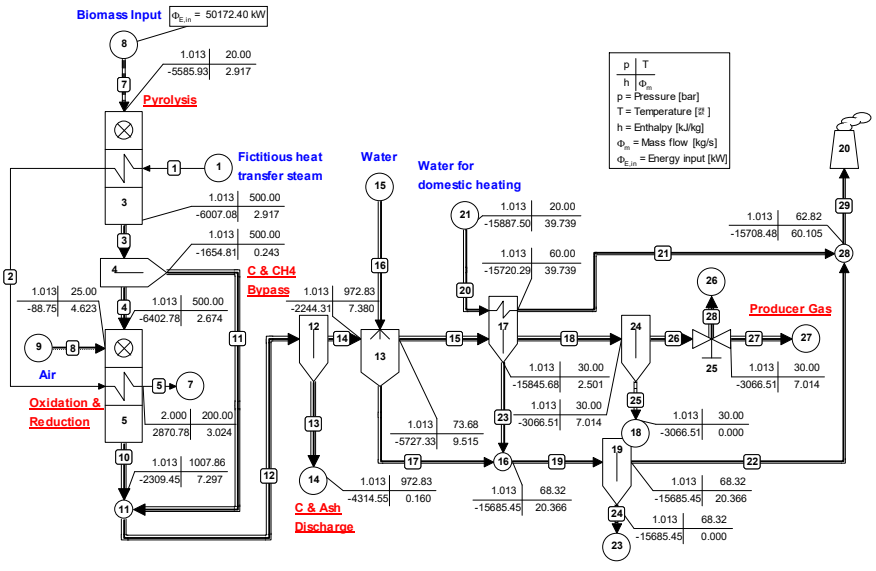

Figure 2. Two-reactor model of biomass downdraft gasifier.

3.2. Three-Reactor Model (Fortunato)

Fortunato et al. upgraded the earlier model by Altafini et al. for better flexibility and accuracy, as shown in Figure 3 [23]. This model includes pyrolysis (gasifier 1), combustion (combustor 11) and reduction (gasifier 17) processes. In the pyrolysis reactor, the theoretical air ratio (air factor) is 0.018 and the pyrolysis temperature is 600 °C. Some amount of heat is transferred from the reduction process by fictitious water flow (source 5 to sink 4) to simulate upstream conduction and radiant heat transfer to satisfy the pyrolysis temperature. The combustion furnace receives most of the processed air, and no air is supplied to the reduction furnace, which is the major difference compared with Altafini's model. This change improves the flexibility of the model by decreasing the number of air injection points, which means the elimination of an unknown variable from the model. The air factor of the oxidation furnace (combustor 11) is fixed at 2. The reduction process is carried out at 850 °C. Afterwards, the separated methane at separator 12 joins at junction 20 to compose the final PG. The fictitious heat exchanger 18 acts combustion air heating to 200 °C by heat exchange with the gasification reactor bed before participating in the oxidation process in combustor 11. Separator 8 separates 5% of non-useful carbon, and separator 21 separates ash and the remaining carbon in the process. The heat loss of the gasifier to the environment is assumed to be 0.5% of the biomass energy, which is 1/10 of the heat loss assumed in Vera et al.'s study.

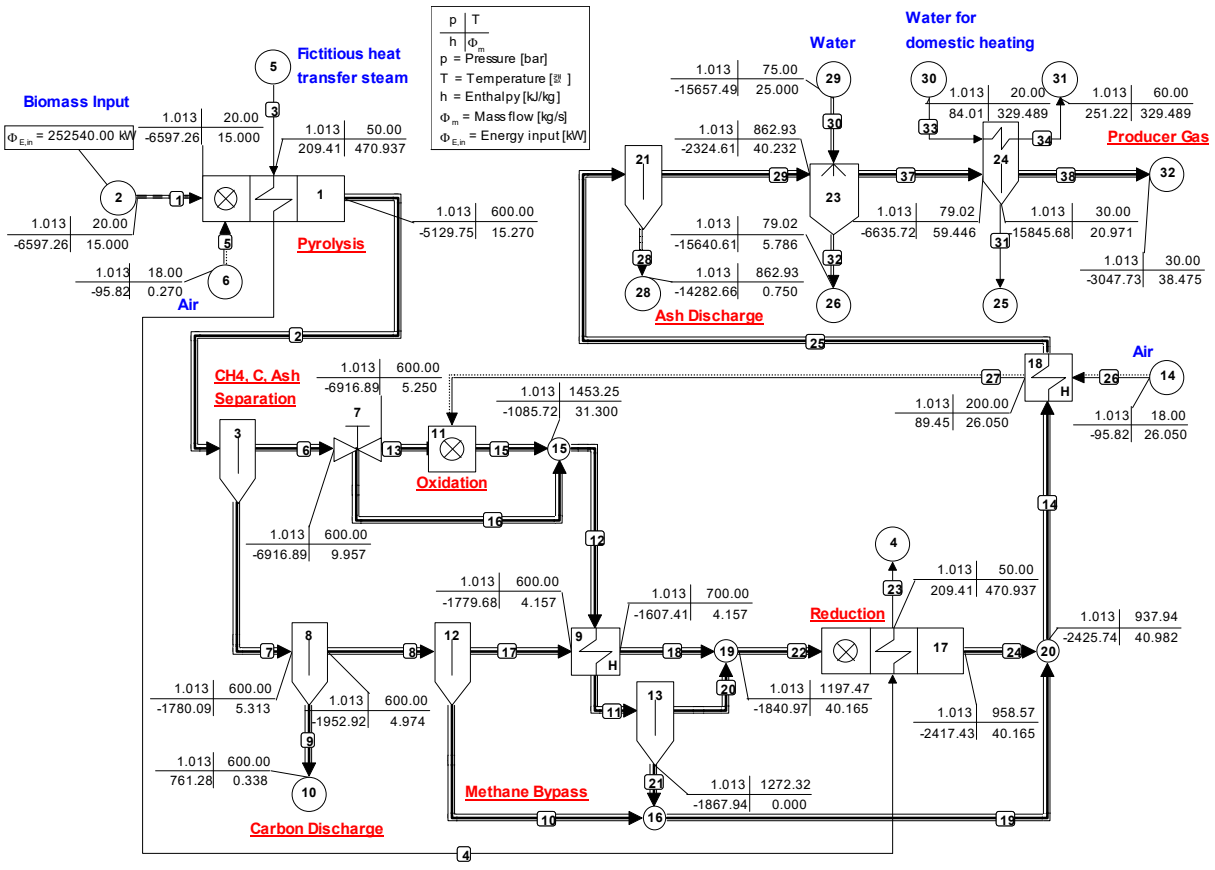

Figure 3. Three-reactor model of biomass downdraft gasifier.

To summarize, the first reactor (gasifier 1) includes moisture evaporation and pyrolysis with limited air supply, the second reactor (combustion 11) simulates partial oxidation of PG, and the third reactor (gasifier 17) simulates the reduction process without air supply.

3.3. Validation of Reconstructed Models and Application for Biochar Production

Table 2 shows the result of comparison between the original models and the reconstructed models of the present study. All the composition data of PG show that the re-constructed models are close to the original models. In particular, LHV of PG and CGE show under 5% error.

Table 2. Comparison results of the reconstruction model and the original literature.

Model	**2 Reactors Model (Vera) [22]**		**3 Reactors Model (Fortunato) [23]**	
Biomass Name	**Olive Pits**		**Depleted Pomace**	
Biomass Composition(wt.%)				
C	44.98		43.22	
H	5.30		5.39	
O	36.86		29.49	
S	0.018		1.68	
N	0.57		0.22	
Water	10.2		5	
Ash	2.06		15	
Total (wt.%)	100		100	
LHV (kJ/kg)	17,200		16,836	
Comparison results	Original	Reconstructed	Original	Reconstructed
Biomass flow rate (kg/s)	0.02917	0.02917	0.15	0.15
Biomass energy (kW)	501.72	501.72	2525.4	2525.4
PG composition (mole fraction)				
H_2	0.163	0.158	0.1719	0.1713
H_2O	0.042	0.0419		0.0419
N_2	0.4382	0.4389	0.487	0.4548
Ar	NR	0.0052	0.0057	0.0053
CO_2	NR	0.0936	0.111	0.1053
CH_4	0.031	0.0296	0.0315	0.0325
CO	0.214	0.2328	0.1923	0.1883
H_2S	NR	0.0001	0.0006	0.0006
LHV of PG (kJ/kg)	5100	5161	4860	4941
PG flow rate (kg/s)	0.069	0.070	NR	0.385
PG energy (kW)	351.9	362.02	NR	1901
Cold gas efficiency (%)	71.2	72.16	76	75.27

NR: not reported.

Differently from the previous research, this study focuses on understanding and maximizing biochar production rate. Using the reconstructed models, biochar production condition is simulated by bypassing more carbon after the pyrolysis process. Meanwhile, the reaction temperature and the reduction gas temperature are kept the same with each original model by adjusting the oxidant flow rate. By this measure, the thermodynamic condition of each reactor is remained the same, whereas the carbon discharge rate in the form of biochar varies.

The maximum carbon separation rate is set by the pyrolysis process. The two and three gasification reactors models have different pyrolysis temperature and oxidant injection rate (air factor), which results in different available carbon discharge rate. The carbon discharge ratio (CDR) is defined as the percent of pure carbon separation after the pyrolysis process. Meanwhile the biochar yield rate is combination of carbon and ash discharge rate as ash is included in biochar. Biochar yield ratio ($Y_{biochar}$), which is the main process performance parameter in this study, is defined by the following equation:

$$Y_{biochar} = \frac{\text{Biochar Yield Rate } \left[\frac{kg}{s}\right]}{\text{Carbon and Ash Input Rate at Dry Condition } \left[\frac{kg}{s}\right]} \quad (1)$$

The cold gas efficiency is defined as Equation (2), which is based on the LHV of biomass and producer gas.

$$CGE = \frac{LHV_{PG} * \dot{m}_{PG}}{LHV_{biomass} * \dot{m}_{biomass}} \quad (2)$$

where $\dot{m}_i$ is the mass flow rate of i material.

3.4. Regression Model of Biochar Production Performance

The results of thermodynamic simulations are used to determine correlation model for relevant performance parameters. The main products of biomass plant are PG and biochar. The quality of PG is evaluated with LHV of PG (LHV_{PG}) and the cold gas efficiency (CGE), which are the two performance parameters. $Y_{biochar}$ is selected as the main variable of the biochar process as LHV_{PG} and CGE strongly related. The other variables that affect the performance were assumed to be LHV of biomass ($LHV_{biomass}$, [kcal/kg]), carbon mass fraction (C_f), moisture mass fraction (W_f), ash mass fraction (A_f) in biomass and temperature of the reduction process (T_r, [K]). The functional relationship between the performance parameters and the variables are assumed in the form of the following equations:

$$LHV_{PG} = a_1 LHV_{biomass}\left(a_2 {Y_{biochar}}^2 + a_3 C_f + a_4 W_f + a_5 A_f + a_6 T_r + a_7\left(\frac{A_f}{W_f}\right)^2 + a_0\right) \quad (3)$$

$$CGE = b_1 Y_{biochar} + b_2 C_f + b_3 W_f + b_4 A_f + b_5 T_r + b_6\left(\frac{A_f}{W_f}\right)^2 + b_0 \quad (4)$$

where a_i and b_i are the coefficients determined by the GRG (generalized reduced gradient) nonlinear solver minimizing the difference between the proposed correlation equations and the full set of simulation results by the thermodynamic model.

4. Results and Discussion

4.1. Process Calculation Results

Figure 4 shows a sample result of the two-reactor model using rice husk as the feed. The heat loss to the environment is a key parameter of the plant performance; however, Vera's model uses 5% of heat loss, whereas Fortunato's model uses 0.5%. Meanwhile, increased heat loss decreases CGE due to increased combustion air supply to maintain the reduction zone temperature. Hence, in this parametric study, the heat loss is assumed to be zero to find out maximum theoretical efficiency. Additionally, the mass flow rate of biomass is fixed to be 1 kg/s, which is from the fact that the thermodynamic efficiency is not the function of scale in an ideal simulation such as this study. As CDR increases at separator 4, the air flow rate (source 9) decreases, and the biochar yield increases (sink 14) accordingly as shown in Table 3. Process simulations for each biomass in Table 1 using two models were carried out by varying CDR in the range of 5% to 100% at separator 4.

Figure 5 shows the sample results of the three-reactor models using rice husks. While the CDR changes, the reduction furnace temperatures of all the simulation remain 850 °C by adjusting pyrolysis gas flow rate at valve 7. Because the stoichiometric equivalence factor (air factor) is fixed at 2, the fuel gas flow rate at valve 7 is directly related with air flow rate at combustor 11. The trends of the results of parametric study in Table 4 is similar between both models. However, overall LHV_{PG} and CGE of three-reactor model is higher than the two-reactor model, which is mainly due to the lower reduction furnace temperature.

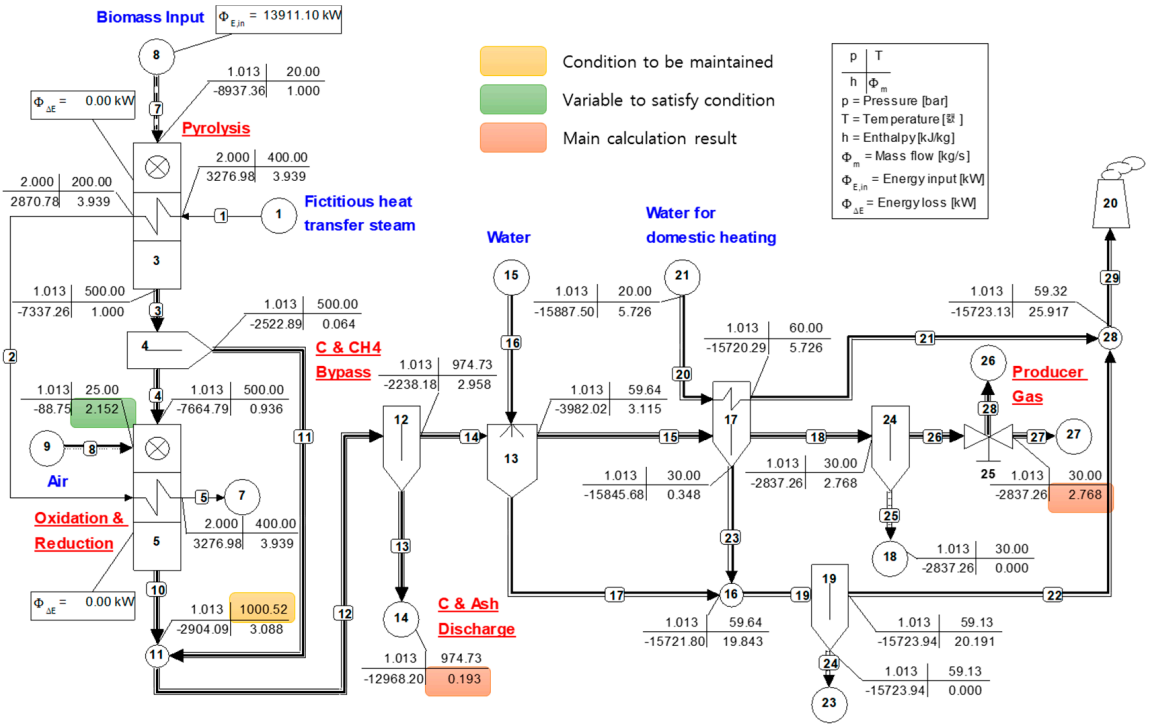

Figure 4. A sample of parametric study of increasing CDR at two-reactor model using rice husk as fuel and CDR 5%.

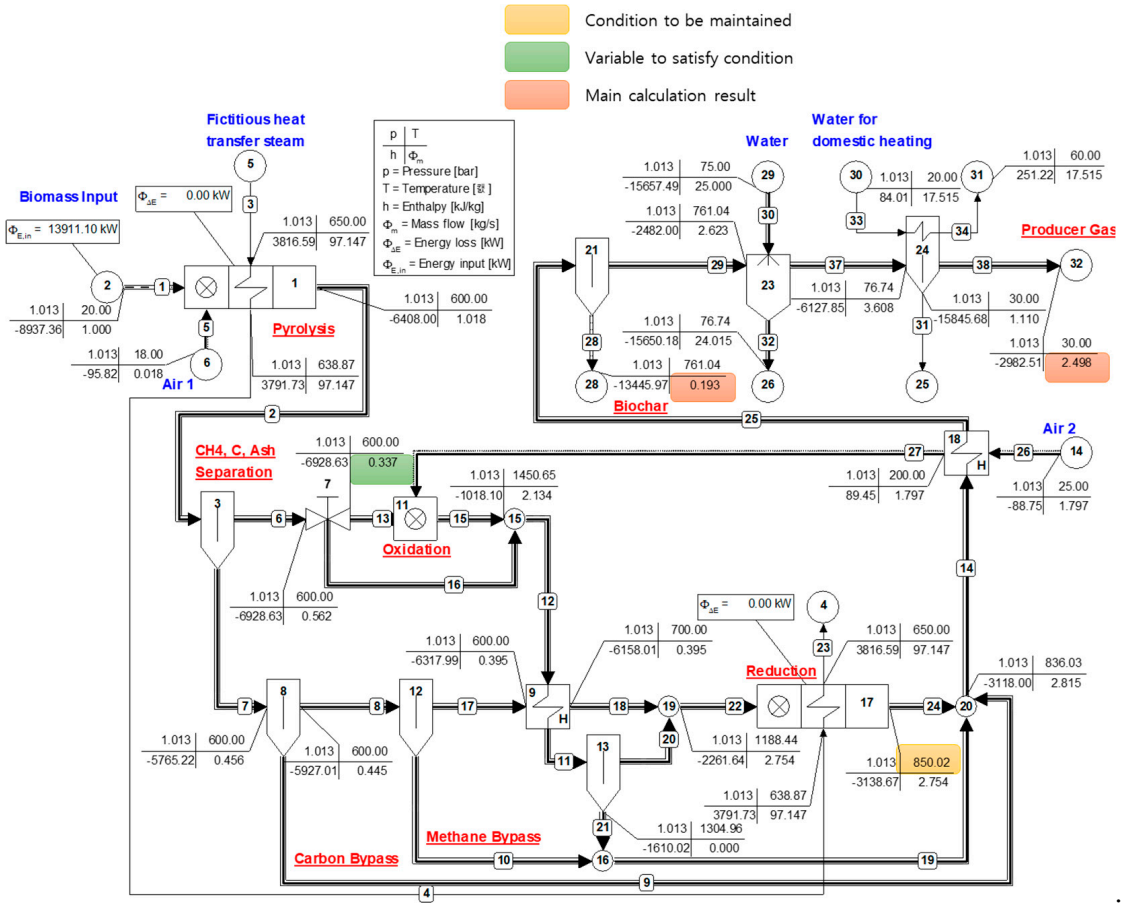

Figure 5. A sample of parametric study of increasing CDR at three-reactor models using rice husk as fuel and CDR 5%.

Table 3. Parametric study result for two-reactor models.

Biomass	Input Variable		Biochar Result			Producer Gas Result				
	CDR	$\dot{m}_{Air}$ (kg/s)	Biochar Rate (kg/s)	$Y_{biochar}$ (%)	PG Rate (kg/s)	(mole %)			LHV_{PG}(kJ/kg)	CGE (%)
						H_2	CH_4	CO		
Rice husk	5%	2.152	0.193	34.46	2.768	10.3	3.1	14.2	3421	68
	20%	1.985	0.229	40.89	2.542	10.2	3.4	12.8	3350	61
	40%	1.764	0.276	49.29	2.400	9.9	3.9	10.8	3234	56
	60%	1.546	0.323	57.68	1.937	9.2	4.5	8.4	3085	43
	80%	1.333	0.371	66.25	1.630	7.6	5.5	5.5	2884	34
Paddy straw	5%	2231	0.219	36.21	2.900	7.8	1.9	15.9	2879	65
	20%	2.031	0.261	43.15	2.634	7.6	2.1	14.3	2739	56
	40%	1.765	0.317	52.41	2.277	7.2	2.4	11.7	2505	45
	60%	1.503	0.374	61.84	1.919	6.2	2.9	8.3	2184	33
	80%	1.245	0.430	71.10	1.557	3.7	3.7	4.0	1720	21
Coconut shell	5%	2.577	0.047	9.31	3.375	8.3	2.0	15.9	2978	67
	20%	2.348	0.095	18.83	3.071	8.2	2.3	14.3	2851	58
	40%	2.044	0.160	31.71	2.663	7.8	2.6	11.8	2639	47
	60%	1.745	0.224	44.39	2.253	6.9	3.2	8.7	2353	35
	80%	1.451	0.288	57.07	1.838	4.7	4.0	4.7	1942	24
Coconut frond	5%	2.325	0.079	16.72	3.032	7.6	2.3	12.6	2609	63
	20%	2151	0.116	24.56	2.798	7.3	2.6	11.1	2473	55
	40%	1.921	0.165	34.93	2.483	6.5	2.9	8.8	2255	45
	60%	1.695	0.215	45.51	2.168	5.2	3.4	6.0	1971	34
	80%	1.473	0.264	55.88	1.849	2.8	4.1	2.7	1595	24
Torrefied arecanut husk	5%	2.692	0.070	12.19	3.534	10.1	2.2	19.8	3707	71
	20%	2.411	0.128	22.30	3.167	10.4	2.4	18.3	3643	63
	40%	2.041	0.206	35.88	2.677	10.6	2.9	15.8	3530	52
	60%	1.676	0.284	49.47	2.184	10.6	3.5	12.7	3369	40
	80%	1.316	0.361	62.88	1.685	9.6	4.6	8.6	3127	29
Cassava stalk	5%	2.305	0.072	15.61	2.979	9.4	3.1	12.6	3087	66
	20%	2.143	0.106	22.99	2.758	9.2	3.4	11.3	2996	60
	40%	1.928	0.153	33.18	2.462	8.7	3.8	9.4	2851	51
	60%	1.716	0.199	43.16	2.164	7.7	4.4	7.1	2670	42
	80%	1.508	0.245	53.13	1.863	5.9	5.2	4.5	2432	33
Cassava rhizome	5%	2.473	0.055	11.17	3.227	10.1	2.8	15.3	3374	69
	20%	2.265	0.099	20.11	2.949	10.1	3.0	13.9	3294	62
	40%	1.992	0.157	31.90	2.577	9.8	3.5	11.8	3159	52
	60%	1.721	0.216	43.88	2.202	9.2	4.1	9.2	2983	42
	80%	1.456	0.274	55.67	1.825	7.5	5.1	6.0	2737	32

Table 4. Parametric study result for three-reactor models.

Biomass	Input Variable		Bio Char Result			Producer Gas Result				
	CDR	$\dot{m}_{Air}$ (kg/s)	Biochar Rate (kg/s)	$Y_{biochar}$ (%)	PG Rate (kg/s)	(mole %)			LHV_{PG} (kJ/kg)	CGE (%)
						H_2	CH_4	CO		
Rice husk	5%	1.815	0.193	34.5	2.498	14.9	3.1	16.4	4303	77
	20%	1.682	0.226	40.4	2.308	15.0	3.4	15.0	4236	70
	40%	1.505	0.270	48.2	2.053	15.1	3.9	12.9	4132	61
	60%	1.331	0.314	56.1	1.795	14.8	4.4	10.5	4003	52
	80%	1.161	0.358	63.9	1.535	13.8	5.3	7.9	3839	42
	100%	0.996	0.402	71.8	1.270	11.6	6.5	4.9	3619	33
Paddy straw	5%	1.893	0.218	36.0	2.615	11.5	1.9	19.0	3695	75
	20%	1.732	0.257	42.5	2.393	11.6	2.1	17.3	3557	66
	40%	1.520	0.309	51.1	2.095	11.5	2.4	14.6	3332	55
	60%	1.310	0.361	59.7	1.794	11.0	2.9	11.4	3038	43
	80%	1.106	0.413	68.3	1.489	9.4	3.6	7.5	2632	31
	100%	0.909	0.466	77.1	1.177	5.1	4.7	2.9	2029	19
Coconut shell	5%	2.201	0.046	9.1	3.065	12.0	2.1	18.5	3755	77
	20%	2.019	0.090	17.84	2.812	12.1	2.3	16.9	3629	68
	40%	1.779	0.149	29.53	2.473	12.1	2.6	14.4	3426	56
	60%	1.542	0.208	41.22	2.130	11.6	3.1	11.4	3161	45
	80%	1.311	0.267	52.91	1.784	10.1	3.8	7.9	2801	33
	100%	1.087	0.327	64.80	1.431	6.5	4.9	3.6	2279	22
Coconut frond	5%	1.974	0.078	16.51	2.747	11.7	2.4	15.0	3376	74
	20%	1.842	0.111	23.50	2.558	11.5	2.6	13.6	3249	67
	40%	1.667	0.154	32.60	2.305	11.1	2.9	11.4	3049	56
	60%	1.496	0.198	41.91	2.051	10.3	3.3	9.0	2801	46
	80%	1.327	0.242	51.23	1.793	8.6	3.9	6.3	2489	36
	100%	1.163	0.285	60.33	1.531	5.6	4.7	3.2	2078	25

Table 4. *Cont.*

Biomass	Input Variable		Bio Char Result		Producer Gas Result				
	CDR	$\dot{m}_{Air}$ (kg/s)	Biochar Rate (kg/s)	$Y_{biochar}$ (%)	PG Rate (kg/s)	(mole %)			LHV_{PG} (kJ/kg)	CGE (%)
						H_2	CH_4	CO		
Torrefied arecanut husk	5%	2.305	0.069	12.02	3.210	13.6	2.2	22.7	4547	80
	20%	2.073	0.125	21.77	2.895	14.1	2.4	20.9	4476	71
	40%	1.767	0.199	34.66	2.473	14.8	2.8	18.2	4357	59
	60%	1.466	0.273	47.55	2.046	15.2	3.4	14.8	4198	47
	80%	1.171	0.347	60.44	1.614	15.0	4.4	10.7	3972	35
	100%	0.888	0.422	73.51	1.172	12.2	6.3	5.5	3606	23
Cassava stalk	5%	1.952	0.071	15.40	2.699	14.0	3.2	14.6	3906	76
	20%	1.828	0.102	22.12	2.519	14.0	3.4	13.3	3822	70
	40%	1.663	0.143	31.01	2.277	13.7	3.8	11.5	3691	61
	60%	1.500	0.185	40.12	2.033	13.2	4.3	9.4	3534	52
	80%	1.340	0.226	49.01	1.786	12.0	5.0	7.1	3339	43
	100%	1.184	0.268	58.12	1.537	9.8	5.9	4.6	3085	34
Cassava rhizome	5%	2.104	0.041	8.33	2.930	14.3	2.8	17.6	4198	78
	20%	1.939	0.095	19.30	2.698	14.5	3.0	16.1	4116	70
	40%	1.720	0.149	30.27	2.384	14.6	3.5	13.8	3989	60
	60%	1.505	0.203	41.24	2.068	14.3	4.0	11.3	3826	50
	80%	1.294	0.258	52.42	1.749	13.4	4.8	8.3	3613	40
	100%	1.089	0.312	63.39	1.423	10.9	6.1	5.0	3318	30

4.2. Producer Gas Characteristics

The species composition result of PG is summarized at Figure 6 depending on $Y_{biochar}$ and feeding biomass. The biomass type has a strong effect on $Y_{biochar}$'s range owing to ash content. Bigger ash content means bigger biochar production rate at the same CDR because ash joins in biochar. The methane fraction of PG is not strongly dependent on the simulation model because methane bypasses the reduction reactor. The mole fraction of methane increases as $Y_{biochar}$ increases due to decreased PG flow rate, whereas the bypassing flow of methane remains the same. The difference in pyrolysis temperature between the models makes the methane composition slightly varying for the same biomass. However, the overall trend depending on $Y_{biochar}$ remains similar. Meanwhile, H_2 and CO mole fraction shows a difference between the simulation models. Even though the trend depending on $Y_{biochar}$ and feed material seems similar, the two-reactor model shows lower concentration of H_2 and CO than the three-reactor model due to a higher reduction zone temperature, which consumes more PG to increase the reduction zone temperature. Additionally, as $Y_{biochar}$ increases, the concentrations of H_2 and CO decrease and they do so more rapidly at higher $Y_{biochar}$. This shows that more volatiles have to be burned to support the reduction zone temperature in the two-reactor models. H_2 and CO concentration in the PG of the two-reactor models is approximately 5% and 3% lower than the three-reactor models, respectively. H_2 concentration shows relatively constant values at varying $Y_{biochar}$ comparing to CO concentration because there is high enough H_2O content in the PG to act as the source of H_2. Meanwhile, the source of CO is carbon which decreases as $Y_{biochar}$ increases; thus, CO concentration declines as $Y_{biochar}$ increases.

Figure 7 shows LHV_{PG} and CGE depending on $Y_{biochar}$ and feeding biomass. LHV_{PG} shows an obvious trend; as $Y_{biochar}$ increases or LHV_0 decreases, LHV_{PG} decreases. Additionally, the two-reactor model has lower LHV_{PG} than the three-reactor model due to higher air supply to maintain the reduction zone temperature. A difference of around 800~1000 kJ/kg in LHV_{PG} is observed between the two simulation models. CGE, which is the main performance parameter of the plant, has a difference of approximately 10% between the two simulation models. It seems that the two biomass groups appear in the CGE chart; rice husk and paddy straw have higher CGE then other biomasses at the same levels of $Y_{biochar}$ due to high ash content in the raw biomass.

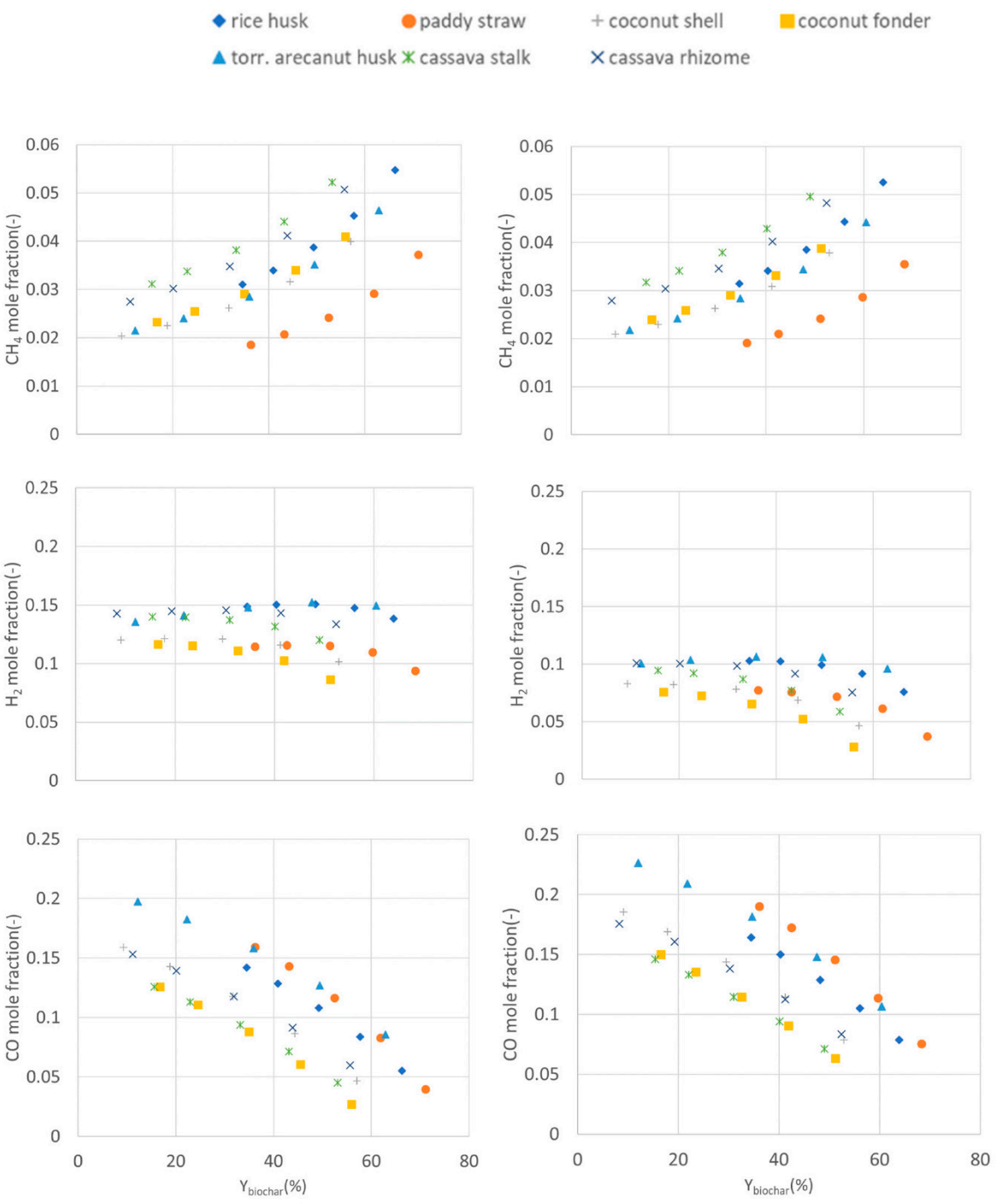

Figure 6. Producer gas composition of each model depending on $Y_{biochar}$: (**a**) two-reactor model, (**b**) three-reactor model.

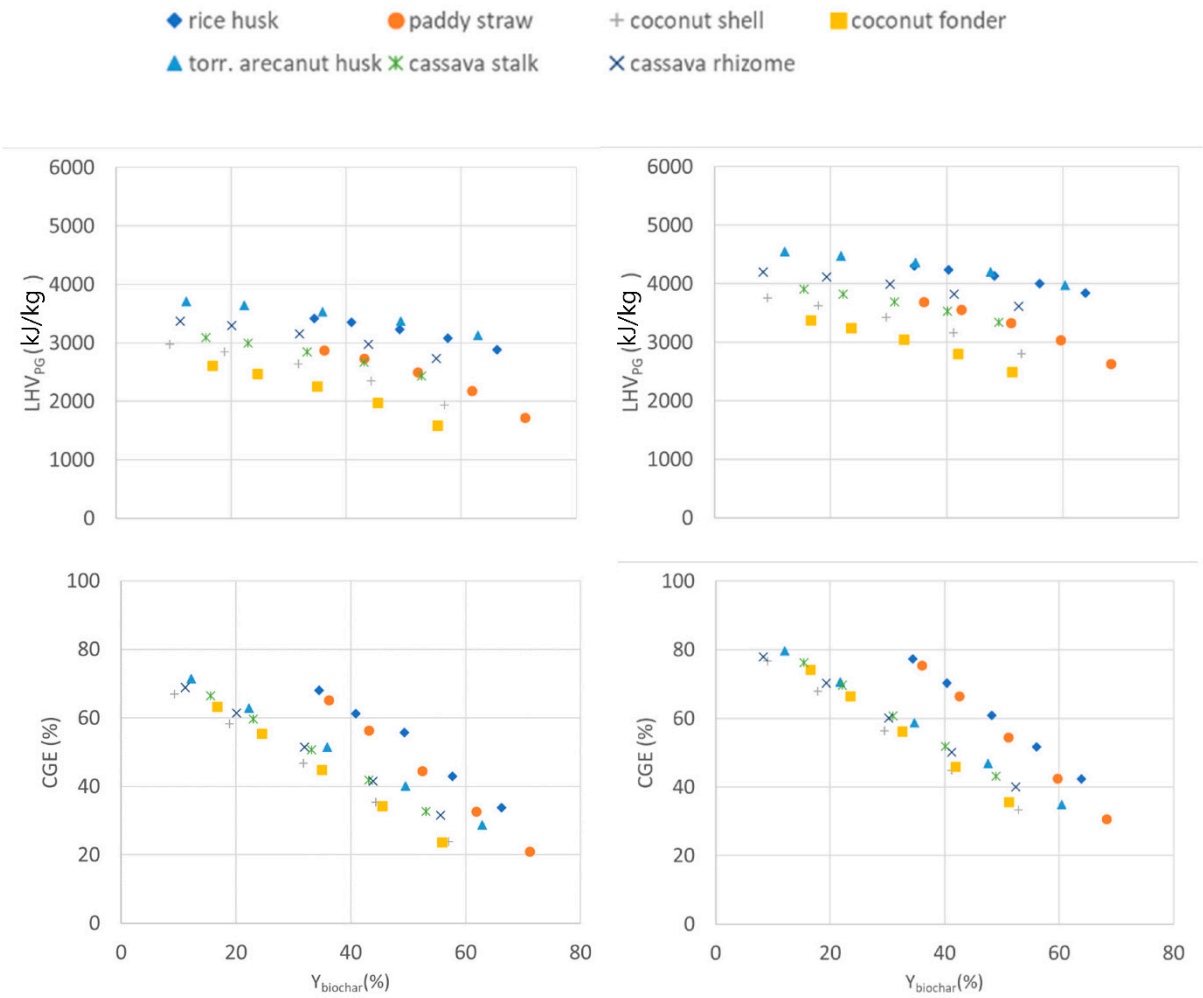

Figure 7. LHV$_{PG}$ and CGE depending on Y$_{biochar}$: (**a**) two-reactor model, (**b**) three-reactor model.

4.3. Regression Models

The performance of the biochar production plant depends on various variables, which makes the prediction difficult. A simplified model to estimate the performance with limited data will decrease the effort to build and simulate all the design and operation conditions of the biomass plant to find out the performance data. Therefore, model equations of LHV$_{PG}$ and CGE model were introduced of the form given in Equations (3) and (4), and the best values of coefficients are derived to be as given in Table 5 by the GRG nonlinear solver. Figure 8 shows the comparison between the simulation results and the regression model equation about LHV$_{PG}$ and CGE. The equations, for LHV$_{PG}$ and CGE give results in good agreement regardless of gasifier models and biomasses with correlations of 98.73% and 96.54%, respectively. However, careful observation on the results of LHV$_{PG}$ shows slightly different trends for each biomass. Torrefied areca nut and coconut fonder, which have the highest and lowest LHV$_0$, respectively, have the steepest and the slowest change in the figure of LHV$_{PG}$. Therefore, bigger errors are expected at the higher and lower zone of LHV$_{PG}$. Other intermediate LHV biomasses show relatively good agreement obtained with the model equation. Meanwhile, the CGE result shows better linear correlation than the *LHV$_{PG}$*.

Table 5. Coefficients of correlation equation for LHV_{PG} and CGE.

		Performance Parameters		
		LHV_{PG}		**CGE**
Model coefficients	a_0	-1.418×10^2	b_0	-1.882×10^{-1}
	a_1	2.491×10^{-3}	b_1	-9.809×10^{-1}
	a_2	-7.358×10^1	b_2	7.979×10^{-1}
	a_3	7.742×10^1	b_3	5.197×10^{-1}
	a_4	1.030×10^2	b_4	1.866
	a_5	2.363×10^2	b_5	4.626×10^{-4}
	a_6	1.533×10^{-1}	b_6	-4.206×10^{-3}
	a_7	-6.738×10^{-1}		
Correlation		96.54%		98.73%
Maximum difference betweensimulationandequation model		520 kJ/kg		8.68%
Standard deviation of difference		124 kJ/kg		1.87%

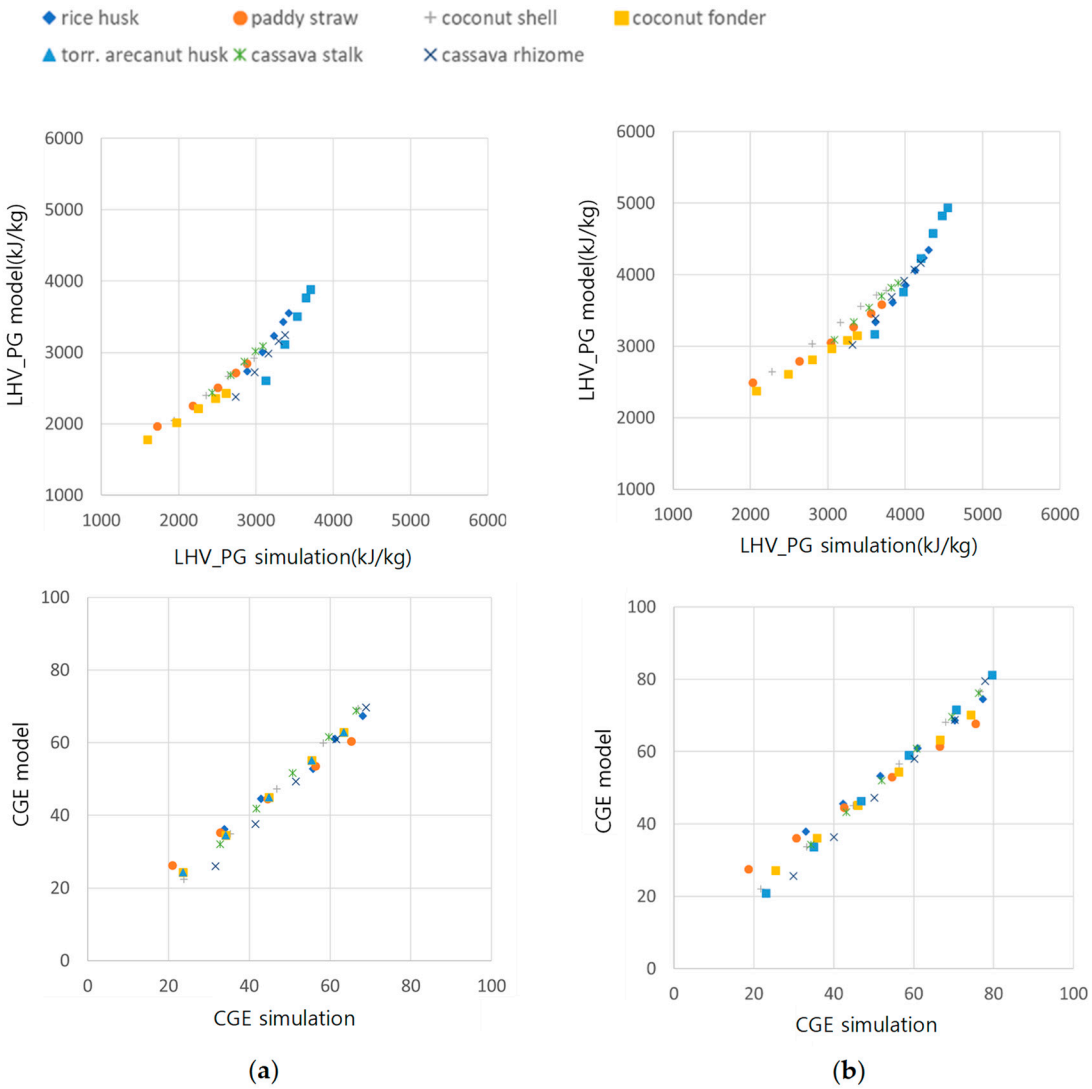

Figure 8. Scatter plot of results for LHV_{PG} and CGE: correlation versus thermodynamic model: (**a**) two-reactor model, (**b**) three-reactor model.

Research on biochar production facilities starts with the gasifier, and until now, focuses on the production yield of fuel gas and liquid, as well as the part on biochar production, has been treated as ancillary. As the importance of biochar in response to climate change has recently been highlighted, research on biochar production methods is being actively conducted. However, most of the studies are at the lab scale in the laboratory, and the studies on the advancement of biochar production in commercial scale are insignificant. The downdraft gasifier is also conducted mainly for lab-scale research, usually batch-type reactors, and the research results of continuous medium-to-large facilities are not common. In Table 6, among the downdraft gasifier studies that have been published so far, the experimental results in continuous facilities including the data of biochar yield were used and the regression model was applied to compare with the actual measurement results [30–36]. A total of 20 measured results were selected, and some data without CGE data or LHV_{PG} were also used for CGE and LHV_{PG} calculations using the provided PG concentration and flow rate. Unfortunately, most of the research results focused on PG production; thus, the ER (equivalence ratio, or air factor) was operated with a focus on stable facility operation in the range of 0.2~0.5. Accordingly, the results of upgrading $Y_{biochar}$ could not be included. In addition, when the measurement of T_r was not accurate, the measurement result of the highest temperature in the gasification reactor was selected as T_r and applied to the regression model.

Figure 9 shows the comparison results about LHV_{PG} and CGE. As expected from Figure 8, CGE shows relatively good agreement between the experiments and the regression model in spite of various biomass, wide scale range and operation condition, whereas the error of LHV_{PG} shows relatively bigger mismatch at above 1000 kcal/kg. However, the regression model based on thermodynamic model with assumption of no heat loss can provide theoretical design and operational information of the advanced biochar production system.

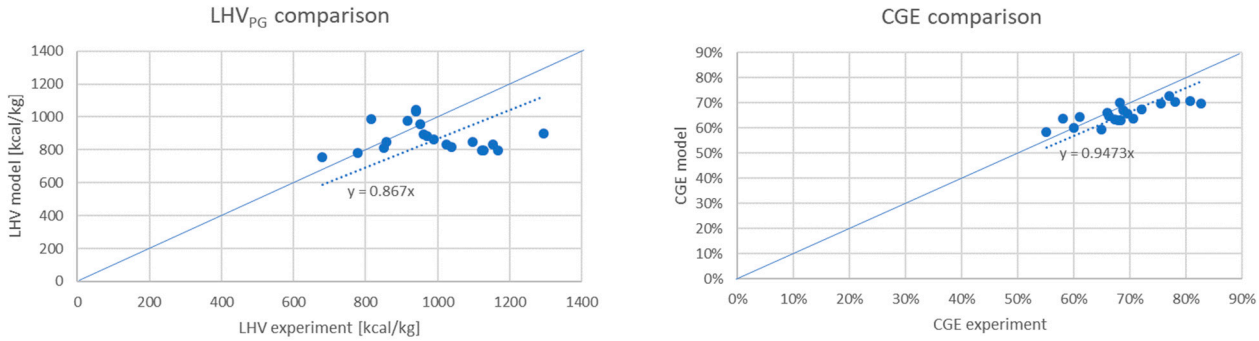

(**a**) (**b**)

Figure 9. Comparison between experimental results with regression model (**a**) LHV_{PG}, (**b**) CGE.

Table 6. Comparison between experimental results and regression model. ( ) parameters of regression model.

Case		**1**	**2**	**3**	**4**	**5**	**6**	**7**	**8**	**9**	**10**	**11**	**12**	**13**	**14**	**15**	**16**	**17**	**18**	**19**	**20**
Reference		[30]	[30]	[30]	[30]	[30]	[31]	[31]	[32]	[33]	[33]	[33]	[33]	[33]	[34]	[35]	[35]	[35]	[36]	[36]	[36]
Biomass feed		Wallnut shell	Wallnut shell	Wallnut shell	Wallnut shell	Wallnut shell	Redwood pellet	Wood chips	Rubber wood chip	Corn cobs	Corn cobs	Corn cobs	Wood pellets	Vine prun-ing	Wood chip	mixed wood chip	Poultry litter	SS/SP	Peach branch	Olive branch	Pine branch
Elementary Analysis																					
	C	46.90%	46.90%	46.90%	46.90%	46.90%	47.11%	46.50%	50.60%	47.60%	47.60%	47.60%	48.91%	50.84%	46.50%	48.77%	43.98%	41.08%	48.06%	46.43%	48.18%
	H	5.96%	5.96%	5.96%	5.96%	5.96%	5.47%	6.30%	6.50%	6.10%	6.10%	6.10%	5.80%	5.82%	5.80%	5.85%	5.16%	5.51%	5.83%	5.63%	5.71%
	N	0.06%	0.06%	0.06%	0.06%	0.06%	0	0	0.20%	0.52%	0.52%	0.52%	0.18%	0.88%	0.20%	0.05%	4.63%	3.77%	0.55%	0.55%	0.15%
	O	46.62%	46.62%	46.62%	46.62%	46.62%	45.00%	44.21%	42.00%	45.78%	45.78%	45.78%	45.11%	42.46%	43.50%	44.52%	31.98%	26.90%	44.03%	44.91%	43.89%
	S	0.46%	0.46%	0.46%	0.46%	0.46%	0	0	0	0	0	0	0	0	0.10%	0.01%	0.75%	0.94%	0	0	0
Proximate Analysis																					
	Ash(dry)	3.65%	3.65%	3.65%	3.65%	3.65%	1.40%	0.80%	0.70%	2.12%	2.12%	2.12%	2.10%	2.62%	3.90%	0.80%	13.5%	21.8%	1.53%	2.48%	2.07%
(W_f)	Moisture	6.56%	6.56%	6.56%	6.56%	6.56%	9.30%	10.1%	14.7%	10.1%	10.1%	10.1%	9.50%	12.5%	21.7%	10.6%	7.60%	4.40%	9.80%	10.6%	9.00%
(LHV_0)	[kcal/kg]	4319	4319	4319	4319	4319	4099	4141	4297	3658	3658	3658	3924	3712	3755	3789	3712	3943	4141	4141	4141
biomass feed	[kg/hr]	8.1	10.2	12.1	12.4	12.9	12	11	18.6	65.6	81.2	81.2	64.1	50.3	55	63	30	28	3.3	3.05	2.5
biochar yield	[kg/hr]	0.44	0.51	0.6	0.73	0.89	0.8	0.4	0.8	4.6	5.8	5.8	6.3	5.3	5.3	3	2.5	4	0.16	0.085	0.128
(Y_biochar)		11.90%	10.96%	10.87%	12.90%	15.12%	15.00%	8.37%	9.83%	16.01%	16.31%	16.31%	21.73%	23.11%	24.42%	10.75%	15.69%	23.76%	10.84%	6.37%	11.2%
(C_f)		42.22%	42.22%	42.22%	42.22%	42.22%	42.13%	41.47%	42.86%	41.89%	41.89%	41.89%	43.33%	43.32%	34.99%	43.25%	35.15%	30.71%	42.69%	40.48%	42.94%
(A_f)		3.41%	3.41%	3.41%	3.41%	3.41%	1.27%	0.72%	0.60%	1.91%	1.91%	1.91%	1.90%	2.29%	3.05%	0.72%	12.47%	20.84%	1.38%	2.22%	1.88%
(Tr)	[K]	1118	1128	1145	1161	1169	1300	1300	1200	1200	1200	1200	1200	1200	1250	1250	1100	1200	1123	1153	1103
CGE_exp		66.19%	65.96%	68.82%	69.51%	70.57%	72.00%	77.00%	68.11%	67.20%	68.35%	67.83%	55.08%	64.83%	60.00%	82.70%	80.70%	75.40%	61.00%	78.00%	58.00%
CGE_model		64.6%	66.0%	66.8%	65.6%	63.8%	67.4%	72.8%	70.0%	63.2%	62.9%	62.9%	58.4%	59.4%	59.9%	69.8%	70.8%	69.6%	64.2%	70.2%	63.7%
Error		2.4%	0.0%	2.9%	5.6%	9.6%	6.4%	5.5%	2.8%	5.9%	8.0%	7.3%	6.1%	8.5%	0.1%	15.6%	12.2%	7.7%	5.3%	10.0%	9.7%
Syngas Vol %																					
	H2	15.42	15.33	15.06	14.86	14.78	14	14	15.5	15.83	17.56	16.6	16.35	17.06	16	16.4	14.55	14	13.2	15	12.1
	CO	17.31	17.24	17.02	16.97	16.87	18	18	19.1	22.46	22.61	22.55	21.29	21.74	19	22.6	17.42	16.4	17.4	17.7	16
	CO_2	6.93	6.99	7.15	7.23	7.29	9	9	11.4	12.33	12.02	11.78	12.39	13.02	17	11.05	13.51	9.2	12.4	13.5	11.4
	CH_4(+HCs)	3.41	3.28	2.98	2.81	2.77	2.5	2.5	1.1	2.92	2.56	2.48	2.72	3.11	2	5.05	1.43	1.18	0.8	1.2	0.2
	N_2(+O_2)	56.93	57.16	57.79	58.13	58.29	56.5	56.5	52.9	46.46	45.25	46.59	47.25	45.07	46	44.9	53.09	59.22	56.2	52.6	60.3
	sum	100	100	100	100	100	100	100	100	100	100	100	100	100	100	100	100	100	100	100	100
Syngas yield	[m^3/hr]								51.9	118	148	150	105	87	130	130	90	87	0	0	0
LHV_PG_exp	[kcal/kg]	1039	1025	989	970	962	939	939	916	1123	1166	1128	1097	1153	952	1293	851	815	778	858	680
LHV_PG_model	[kcal/kg]	816	834	863	885	893	1032	1044	976	798	797	797	845	833	955	897	811	987	783	847	756
Error	0	25.8%	23.1%	17.2%	14.8%	13.9%	7.5%	11.1%	6.6%	28.9%	31.6%	29.3%	22.9%	27.8%	0.3%	30.6%	4.7%	21.1%	0.6%	1.3%	11.2%

5. Conclusions

In the present study, two different biomass gasifier models using thermodynamic software were evaluated for application to biochar production process. The two simulation models were rebuilt, the implementation verified and subsequently a parametric study on biochar production has been carried out. Furthermore, correlations for LHV_{PG} and CGE were formulated based on the thermodynamic simulation to supply simplified prediction correlations.

The two-reactor model and the three-reactor model were reconstructed and showed the same methane concentration trend, depending on $Y_{biochar}$ and biomass characteristics. However, H_2 and CO concentration as well as LHV_{PG} show differences due to the difference in reduction zone temperature. The two-reactor model has a higher reduction zone temperature which requires more combustion heat from PG. However, their trends depending on $Y_{biochar}$ for each biomass show a similar pattern. Hence, these two different models are expected to generate similar results.

Examining the thermodynamic simulation model results, the performance parameters include multiple independent variables, which makes the estimation process difficult and requires professional knowledge on the simulation. Based on a selection of independent variables including biochar yield ($Y_{biochar}$), $LHV_{biomass}$, reduction zone temperature (T_r), biomass contents of ash (A_f), water (W_f) and carbon (C_f), the correlation equations from regression analysis show a good match with the simulation results, which show 96.54% and 98.73% correlations for LHVPG and CGE, respectively. In spite of variations in biomass, scale and operation conditions, the correlation equations are supposed to supply a useful information for design, operation and feasibility evaluation of a biochar production system. However, because the results are based on no heat loss assumption of the thermodynamic simulation, it should be considered as theoretical information.

Author Contributions: Conceptualization, D.S.; methodology, D.S.; resources, A.F.; data curation, A.F.; writing—original draft preparation, A.F.; writing—review and editing, D.R.; visualization, T.W.; supervision, W.d.J.; project administration, P.V.A.; funding acquisition, D.S. All authors have read and agreed to the published version of the manuscript.

Funding: This research was funded by KETEP (Korea Institute of Energy Technology Evaluation and Planning) No. 202003040030090 and KEIT (Korea Evaluation Institute of Industrial Technology) No. 20213030040550.

Institutional Review Board Statement: Not applicable.

Informed Consent Statement: Not applicable.

Data Availability Statement: Not applicable.

Conflicts of Interest: The authors declare no conflict of interest.

References

1. Li, L.; Yao, Z.; You, S.; Wang, C.-H.; Chong, C.; Wang, X. Optimal design of negative emission hybrid renewable energy systems with biochar production. *Appl. Energy* **2019**, *243*, 233–249. [CrossRef]
2. Mendiara, T.; García-Labiano, F.; Aba, A.; Gayán, P.; de Diego, L.F.; Izquierdo, M.T.; Adánez, J. Negative CO_2 emissions through the use of biofuels in chemical looping technology: A review. *Appl. Energy* **2018**, *242*, 657–684. [CrossRef]
3. Rubin, E.S.; Davison, J.E.; Herzog, H.J. The cost of CO_2 capture and storage. *Int. J. Greenh. Gas Control* **2015**, *40*, 378–400. [CrossRef]
4. Volperts, A.; Plavniece, A.; Dobele, G.; Zhurinsh, A.; Kruusenberg, I.; Kaare, K.; Locs, J.; Tamasauskaite-Tamasiunaite, L.; Norkus, E. Biomass based activated carbons for fuel cells. *Renew. Energy* **2019**, *141*, 40–45. [CrossRef]
5. Liua, Y.; Paskeviciusa, M.; Wanga, H.; Parkinsona, G.; Vederb, J.; Huc, X.; Lia, C.Z. Role of O-containing functional groups in biochar during the catalytic steam reforming of tar using the biochar as a catalyst. *Fuel* **2019**, *253*, 441–448. [CrossRef]
6. Zhang, Z.; Zhu, Z.; Shen, B.; Liu, L. Insights into biochar and hydrochar production and applications: A review. *Energy* **2019**, *171*, 581–598. [CrossRef]
7. Guo, F.; Peng, K.; Liang, S.; Jia, X.; Jiang, X.; Qian, L. Evaluation of the catalytic performance of different activated biochar catalysts for removal of tar from biomass pyrolysis. *Fuel* **2019**, *258*, 116–204. [CrossRef]
8. Lee, J.; Kim, K.H.; Kwon, E.E. Biochar as a Catalyst. *Renew. Sustain. Energy Rev.* **2017**, *77*, 70–79. [CrossRef]

9. Wang, J.; Wang, S. Preparation, modification and environmental application of biochar: A review. *J. Clean. Prod.* **2019**, *227*, 1002–1022. [CrossRef]
10. Motta, I.L.; Miranda, N.T.; Filho, R.M.; Maciel, M.R.W. Biomass gasification in fluidized beds: A review of biomass moisture content and operating pressure effects. *Renew. Sustain. Energy Rev.* **2018**, *94*, 998–1023. [CrossRef]
11. Susastriawan, A.A.P.; Saptoadi, H.; Purnomo. Small-scale downdraft gasifiers for biomass gasification: A review. *Renew. Sustain. Energy Rev.* **2017**, *76*, 989–1003. [CrossRef]
12. Safarian, S.; Unnþorsson, R.; Richter, C. A review of biomass gasification modelling. *Renew. Sustain. Energy Rev.* **2019**, *110*, 378–391. [CrossRef]
13. Cha, J.S.; Park, S.H.; Jung, S.-C.; Ryu, C.; Jeon, J.; Shin, M.; Park, Y.-K. Production and utilization of biochar: A review. *J. Ind. Eng. Chem.* **2016**, *40*, 1–15. [CrossRef]
14. Molino, A.; Chianese, S.; Musmarrab, D. Biomass gasification technology:The state of the art overview. *J. Energy Chem.* **2016**, *25*, 10–25. [CrossRef]
15. Bunchan, S.; Poowadin, T.; Trairatanasirichai, K. A Study of Throat Size Effect on Downdraft Biomass Gasifier Efficiency. *Energy Procedia* **2017**, *138*, 745–750. [CrossRef]
16. Siddiqui, H.; Thengane, S.K.; Sharma, S.; Mahajani, S.M. Revamping downdraft gasifier to minimize clinker formation for high-ash garden waste as feedstock. *Bioresour. Technol.* **2018**, *266*, 220–231. [CrossRef]
17. Bhoi, P.R.; Huhnke, R.L.; Kumar, A.; Thapa, S.; Indrawan, N. Scale-up of a downdraft gasifier system for commercial scale mobile power generation. *Renew. Energy* **2018**, *118*, 25–33. [CrossRef]
18. Hrbek, J. *Status Report on Thermal Biomass Gasification in Countries Participating in IEA Bioenergy Task 33*; Vienna University of Technology: Vienna, Austria, 2016; p. 69.
19. Situmorang, Y.A.; Zhao, Z.; Yoshida, A.; Abudula, A.; Guan, G. Small-Scale Biomass Gasification Systems for Power Generation (<200 kW Class): A Review. *Renew. Sustain. Energy Rev.* **2020**, *117*, 109486. [CrossRef]
20. Niu, Y.; Lv, Y.; Lei, Y.; Liu, S.; Liang, Y.; Wang, D.; Hui, S. Biomass torrefaction: Properties, applications, challenges, and economy. *Renew. Sustain. Energy Rev.* **2019**, *115*, 109395. [CrossRef]
21. Altafini, C.R.; Wander, P.R.; Barreto, R.M. Prediction of the working parameters of a wood waste gasifier through an equilibrium model. *Energy Convers. Manag.* **2003**, *44*, 2763–2777. [CrossRef]
22. Vera, D.; Mena, B.; Jurad, F.; Schories, G. Study of a downdraft gasifier and gas engine fueled with olive oil industry wastes. *Appl. Therm. Eng.* **2013**, *51*, 119–129. [CrossRef]
23. Fortunato, B.; Brunetti, G.; Camporeale, S.M.; Torresi, M.; Fornarelli, F. Thermodynamic model of a downdraft gasifier. *Energy Convers. Manag.* **2017**, *140*, 281–294. [CrossRef]
24. Makwana, J.P.; Pandey, J.; Mishra, G. Improving the properties of producer gas using high temperature gasification of rice husk in a pilot scale fluidized bed gasifier (FBG). *Renew. Energy* **2019**, *130*, 943–951. [CrossRef]
25. Grover, S.; Kathuria, R.S.; Kaur, M. Energy Values and Technologies for Non woody Biomass: As a clean source of Energy. *IOSR J. Electr. Electron. Eng.* **2012**, *1*, 10–14. [CrossRef]
26. Werther, J.; Saenger, M.; Hartge, E.-U.; Ogada, T.; Siagi, Z. Combustion of agricultural residues. *Prog. Energy Combust. Sci.* **2000**, *26*, 1–27. [CrossRef]
27. Sadig, H.; Sulaiman, S.A.; Moni, M.N.Z.; Anbealagan, L.D. Characterization of date palm frond as a fuel for thermal conversion processes. *UTP-UMP Symp. Energy Syst.* **2017**, *137*, 01002. [CrossRef]
28. Gogoi, D.; Bordoloi, N.; Goswami, R.; Narzari, R.; Kataki, R. Effect of torrefaction on yield and quality of pyrolytic products of arecanut husk: An agro-processing wastes. *Bioresour. Technol.* **2017**, *242*, 36–44. [CrossRef]
29. Pattiya, A.; Titiloye, J.O.; Bridgwater, A.V. Fast Pyrolysis of Agricultural Residues from Cassava Plantation for Bio-oil Production. In Proceedings of the 2nd Joint International Conference on "Sustainable Energy and Environment (SEE 2006)", Bangkok, Thailand, 21–23 November 2006; C-007(P). 2006. Available online: https://www.researchgate.net/profile/Tony-Bridgwater-2/publication/242696651_Fast_Pyrolysis_of_Agricultural_Residues_from_Cassava_Plantation_for_Bio-oil_Production/links/551a6a200cf2f51a6fea438e/Fast-Pyrolysis-of-Agricultural-Residues-from-Cassava-Plantation-for-Bio-oil-Production.pdf (accessed on 1 October 2022).
30. Mazhkoo, S.; Dadfar, H.; Sina, M.; Hashemi, H.; Pourali, O. A comprehensive experimental and modeling investigation of walnut shell gasification process in a pilot-scale downdraft gasifier integrated with an internal combustion engine. *Energy Convers. Manag.* **2021**, *231*, 113836. [CrossRef]
31. Li, C.Y.; Shen, Y.; Wu, J.Y.; Dai, Y.J.; Wang, C. Experimental and modeling investigation of an integrated biomass gasifier–engine–generator system for power generation and waste heat recovery. *Energy Convers. Manag.* **2019**, *199*, 112023. [CrossRef]
32. Jayah, T.H.; Aye, L.; Fuller, R.J.; Stewart, D.F. Computer simulation of a downdraft wood gasifier for tea drying. *Biomass Bioenergy* **2003**, *25*, 459–469. [CrossRef]
33. Biagini, E.; Barontini, F.; Tognotti, L. Development of a bi-equilibrium model for biomass gasification in a downdraft bed reactor. *Bioresour. Technol.* **2016**, *201*, 156–165. [CrossRef] [PubMed]

34. Son, Y.; Yoon, S.J.; Kim, Y.K.; Lee, J. Gasification and power generation characteristics of woody biomass utilizing a downdraft gasifier. *Biomass Bioenergy* **2011**, *35*, 4215–4220. [CrossRef]
35. Striūgas, N.; Zakarauskas, K.; Džiugys, A.; Navakas, R.; Paulauskas, R. An evaluation of performance of automatically operated multi-fuel downdraft gasifier for energy production. *Appl. Therm. Eng.* **2014**, *73*, 1151–1159. [CrossRef]
36. Pedroso, D.T.; Aiello, R.C.; Conti, L.; Mascia, S. Biomass Gasification on a New Really Tar Free Downdraft Gasifier, University of Sassari, Department of Chemistry, Thermal Process of Biomass Research Group 2015. Available online: https://periodicos.unitau.br/ojs/index.php/exatas/article/view/345/497 (accessed on 1 October 2022).